

Improved simulation of water vapour and clear-sky radiation using 24 hour forecasts from ERA40

By RICHARD P. ALLAN^{*}, *ESSC, University of Reading, Reading, UK*

ABSTRACT

Monthly mean water vapour and clear-sky radiation extracted from the European Centre for Medium Range Weather Forecasts 40-year reanalysis (ERA40) forecasts are assessed using satellite observations and additional reanalysis data. There is a marked improvement in the interannual variability of column integrated water vapour (CWV) over the oceans when using the 24 hour forecasts compared with the standard 6 hour forecasts products. The spatial distribution of CWV are well simulated by the 6 hour forecasts; using the 24 hour forecasts does not degrade this simulation substantially and in many cases improves on the quality. There is also an improved simulation of clear-sky radiation from the 24 hour forecasts compared with the 6 hour forecasts based on comparison with satellite observations and empirical estimates. Further work is required to assess the quality of water vapour simulation by reanalyses over land regions. Over the oceans, it is recommended that 24 hour forecasts of CWV and clear-sky radiation are used in preference to the standard 6 hour forecast products from ERA40.

1. Introduction

Tropospheric water vapour and clear-sky radiative cooling are important components of the atmospheric hydrological cycle (e.g. Stephens *et al.* 1994). Accurate representation of these quantities is critical for climate prediction and therefore model simulation of these diagnostics must be continually evaluated. Satellite measurements and ground-based observations offer a powerful means of assessing model skill. However, where observational sampling is limited, reanalyses present an additional powerful source of information on the state of the atmosphere.

Previously, it has been shown that the European Centre for Medium Range Weather Forecasts 40-year reanalysis (ERA40) provides an accurate spatial representation of water vapour and clear-sky radiation but that interannual variability is poor (Allan *et al.* (2004), Trenberth *et al.* (2005)). Recently, Uppala *et al.* (2005) showed an improved representation of column integrated water vapour (CWV) and precipitation simulated by 24-hour forecasts from ERA40 compared with the standard 6-hourly analysis products over the equatorial oceans. The present study seeks to assess the global performance of the 24 hour forecasts of water vapour and clear-sky radiation from ERA40 for the period 1979–2001.

2. Data

Monthly-mean column integrated water vapour (CWV), clear-sky outgoing longwave radiation (OLRc) and surface net longwave radiation (SNLc) from ERA40 are sampled on a 2.5×2.5 degree spatial grid over the period 1979–2001. The 6-hour and 24-hour forecasts are used to generate CWV

while the clear-sky radiation diagnostics are available as accumulations over 0–6 hours and 24–36 hours. In addition to ERA40, data from the National Center for Environmental Prediction/National Center for Atmospheric Research reanalysis (NCEP; Kalnay *et al.* 1996) for 1979–2004 on a 1.875 longitude by 1.9 degree latitude spatial grid were acquired. Release 2 of the Surface Radiation Budget (SRB; Stackhouse *et al.* 1999) project provided clear-sky fluxes on a 1×1 degree spatial grid from 1983–1994; the clear-sky SRB fluxes are determined by reanalysis data.

Observations of column integrated water vapour over the ice-free ocean were provided by the Scanning Multi-channel Microwave Radiometer (SMMR; Wentz and Francis 1992) for the period 1979–84 and from Version 5 of the Special Sensor Microwave Imager (SSM/I Wentz 1997) for the period 1987–99. The SMMR data were bi-linearly interpolated from a 1×1 degree resolution to the ERA40 grid. SSM/I data were provided on a 0.25×0.25 degree grid and averaged up to the 2.5×2.5 degree ERA40 grid only where the 2.5×2.5 grid-box contained more than 70% data coverage.

The SMMR and SSM/I data were also used as input to an empirical formula (Prata 1996) to provide an observationally derived estimate of SNLc variability. Calculations were conducted on a 1×1 degree resolution grid using also sea surface temperature data from the Hadley Centre global sea-Ice and Sea Surface Temperature dataset (HadISST; Rayner *et al.* 2003)) and a sea minus air temperature climatology from da Silva *et al.* (1994); for further details, see Allan (2006).

Finally, satellite observations of OLRc were used from multiple platforms: the Earth Radiation Budget Satellite (ERBS; 1985–89), the Scanner for Radiation Budget instru-

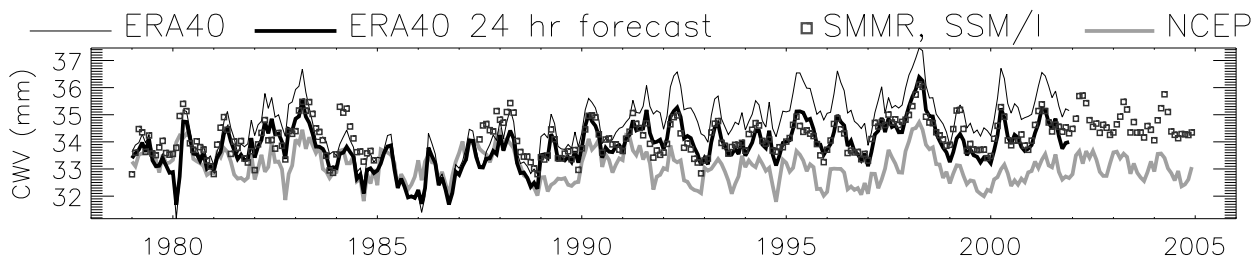


Fig 1. Time-series of monthly mean column integrated water vapour (CWV) over the oceans (40°S - 40°N).

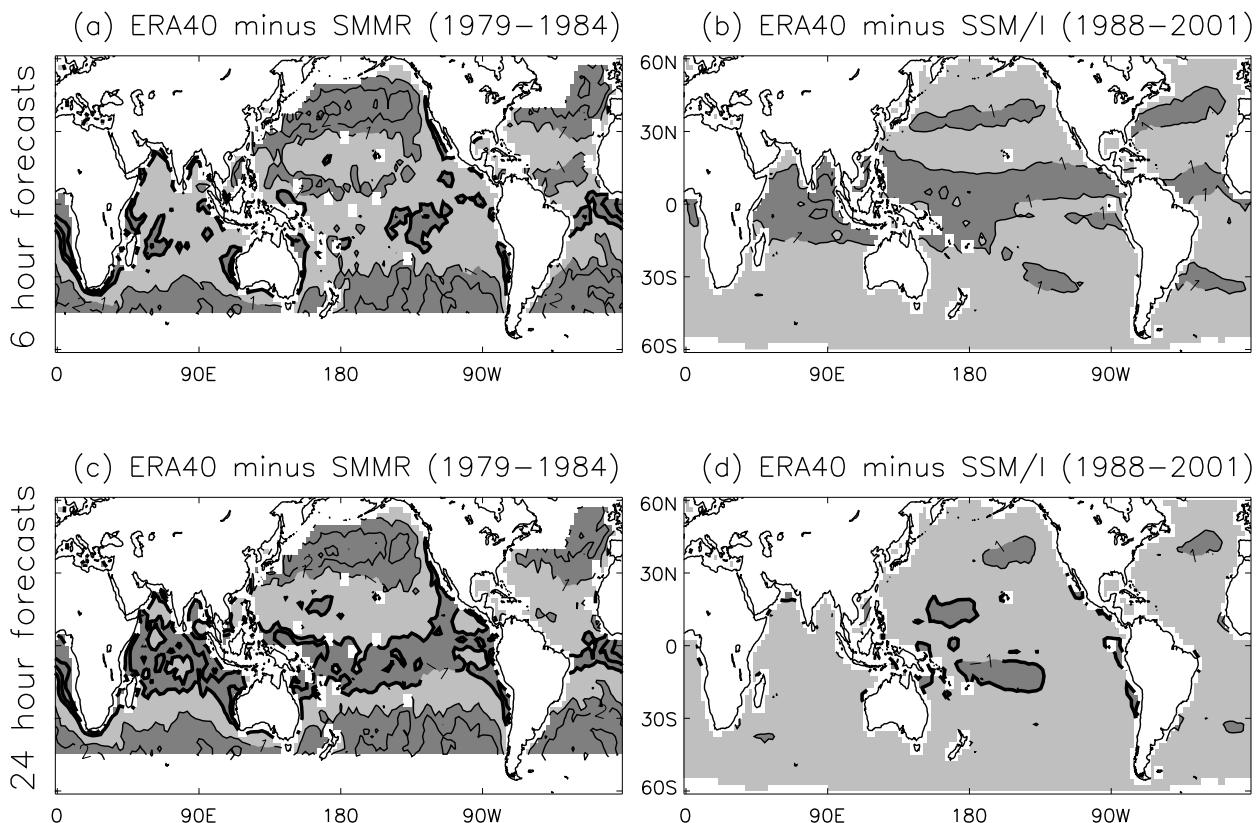


Fig 2. Differences in column integrated water vapour (CWV) over the ocean (Wm^{-2}): ERA40 6-hour forecasts minus (a) SMMR for 1979-84 and (b) SSM/I for 1988-2001 and ERA40 24-hour forecasts minus (c) SMMR and (d) SSM/I.

ment (ScaRab; 1994/5), and the Clouds and the Earth's Radiant Energy System (CERES) instruments (Version ES4_TRMM-PFM_EDITION2_015013 for 1998 and Version ES4_Terra-FM1_Edition2_024026 for 2000-2004). These data are described in Wielicki *et al.* (2002) and references therein.

3. Column integrated water vapour

Uppala *et al.* (2005) demonstrated an improved simulation of column integrated water vapour over the tropical oceans by the 24-hour forecasts from ERA40 compared to the 6-hour forecasts. Figure 1 confirms this for a larger domain (40°S - 40°N). Overestimates by the 6-hour forecasts of order 1 mm ($\sim 3\%$) compared with the satellite observations are evident for the periods 1982-83 and 1989-2001; these discrepancies are substantially reduced using the 24-hour forecasts. Both ERA40 products simulate lower CWV than SMMR

in 1984 and SSM/I during 1987 with the differences being slightly larger for the 24-hour forecasts. While the NCEP data accurately reproduces the observed interannual variability in CWV (e.g. Allan *et al.* 2004), the mean is about 3% lower than the satellite measurements for the low-latitude ocean. This may relate to the unrealistic spatial representation of water vapour provided by NCEP (Allan *et al.* 2004).

The time-series analysis above was also repeated for the 50°S - 50°N region (not shown). This gave similar results to Fig. 1 but with poorer agreement between ERA40 and SMMR data, explained in part by the increased occurrence of missing satellite data at higher latitudes. The effect of the missing data on these comparisons was investigated further by performing an alternative averaging strategy. Rather than calculating an area-weighted average of all non-missing oceanic data as in Fig. 1, ocean-means were also calculated by first computing zonal means from the non-missing data and subsequently performing an area-weighted aver-

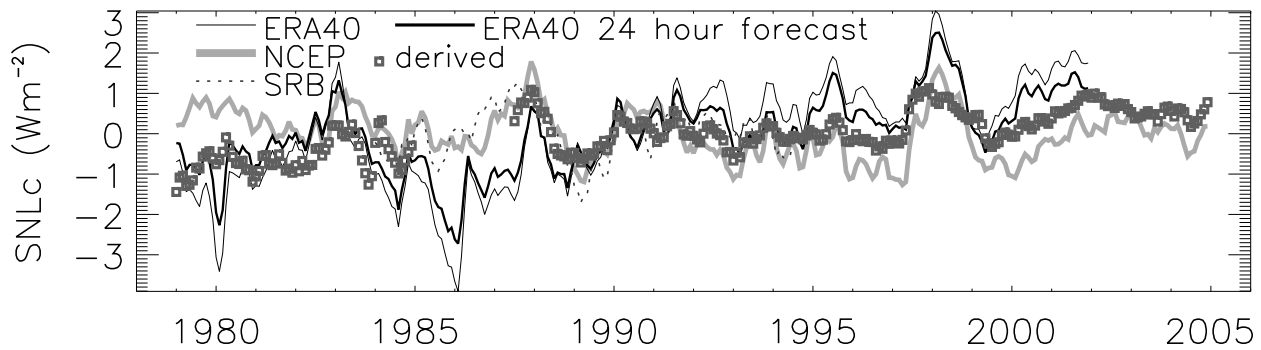


Fig 3. Monthly-mean anomaly time series of clear-sky surface net longwave radiative flux to the ocean (40°S - 40°N). The mean seasonal cycle for each time-series is subtracted and a 3 month running mean applied.

age of the zonal means for each dataset (not shown). While the differing methods alter the seasonal variability substantially, the interannual anomalies (calculated by removing the mean seasonal cycle) and the inter-dataset differences are not strongly affected. For the SMMR and SSM/I data, the different averaging methods cause differences in the inter-annual anomalies of less than 0.13 mm ($\sim 0.4\%$) for all but November-December 1982 and December 1987, due to increased quantities of missing data, where differences were still below 1% of the mean CWV.

While the 24-hour forecast data from ERA40 substantially improves the simulated variability in water vapour, it is important to demonstrate that these products maintain the robust spatial structure in humidity fields displayed by the 6-hour forecast products. Figure 2 shows differences in CWV (ERA40 minus satellite data) for the 6-hour and 24-hour forecasts. For both products, differences are larger for comparisons with the SMMR data compared to the ERA40 minus SSM/I differences which are generally smaller than 2 mm . This is unsurprising since SSM/I radiance data is assimilated by ERA40. The 6-hour forecasts overestimate CWV over mid-latitudes by $\sim 2\text{ mm}$ and underestimate by a smaller magnitude over equatorial regions compared to SMMR (Fig. 2a). Similar results are found for the 24-hour forecasts (Fig. 2c), apart from over equatorial regions where the negative bias becomes more widespread.

The ERA40 6-hour forecasts overestimate CWV by about $1\text{-}2\text{ mm}$ over the tropics compared with SSM/I (Fig. 2b). The 24-hour forecasts underestimate CWV over the same region but by a smaller magnitude (Fig. 2d). Over the vast majority of the ice-free oceans, the 24-hour forecasts from ERA40 reproduce the SSM/I observations to within the expected rms inter-calibration error of 1.2 mm (Wentz 1997). In summary, the high quality simulation of CWV distribution provided by ERA40 6-hour forecasts are maintained and in some cases improved by using the 24-hour forecasts with the possible exception of the equatorial belt for the 1979-84 comparisons. Combined with the improved representation of interannual variability, the 24-hour forecasts of CWV are indeed superior in quality to the 6-hour forecasts as indicated by Uppala *et al.* (2005).

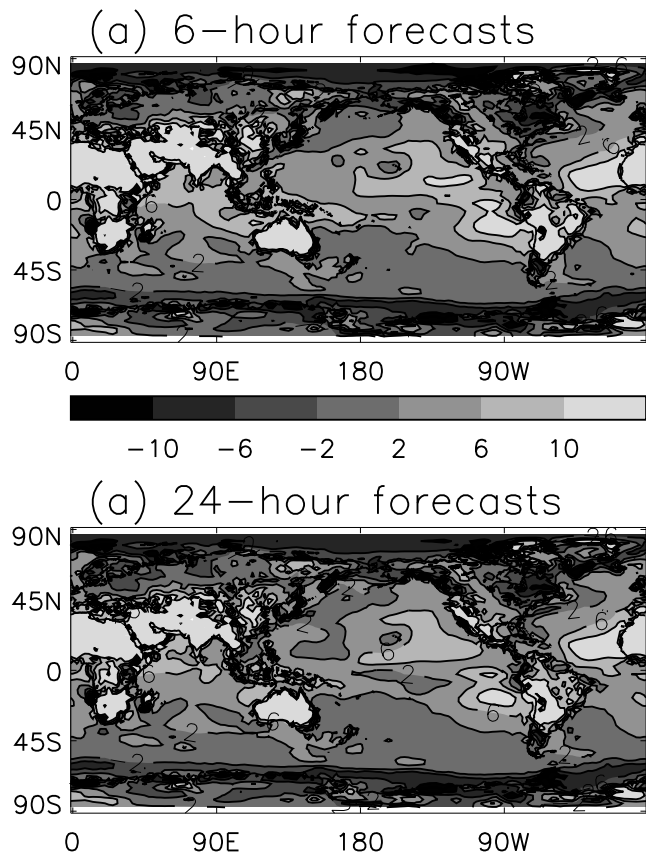


Fig 4. Differences in clear-sky surface net downward longwave radiation (SNLc) over the period 1984-94 for (a) ERA40 0-6 hour forecast minus SRB, (b) ERA40 24-36 hour forecast minus SRB (units: Wm^{-2})

4. Clear-sky Radiation

The improved simulation of water vapour suggests that a more robust representation of clear-sky radiation may also be attained by using the 24-36 hour forecast accumulations from ERA40.

4.1. Clear-sky surface net longwave radiation

Figure 3 displays time series of the clear-sky surface downward net longwave radiation (SNLc) over the low-latitude

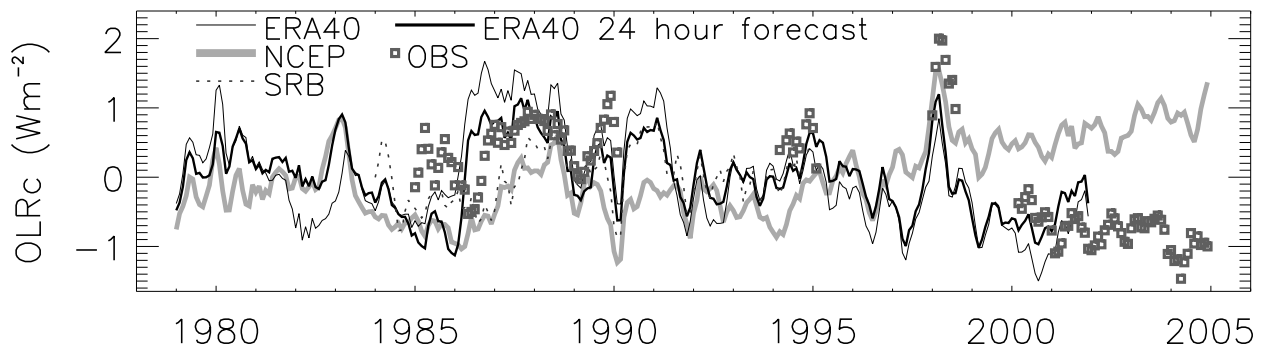


Fig 5. Monthly-mean anomaly time series of clear-sky outgoing longwave radiation (OLRc) for the ocean region 40°S-40°N. The mean seasonal cycle for each time-series is subtracted and a 3 month running mean applied.

oceans. The mean SNLc over this domain is approximately -70 to -80 Wm^{-2} (a surface cooling); thus positive SNLc anomalies signify a heating of the surface (or a reduction in net cooling). The large seasonal cycle is calculated separately for each dataset and removed from the series and a 3-month running mean applied to highlight interannual anomalies. In addition to the ERA40 forecasts and NCEP data, also shown are data from SRB and derived from the combination of SMMR-SSM/I, HadISST and da Silva (Allan 2006).

All datasets reproduce an increase in SNLc anomalies (surface heating) during the El Niño warm events of 1982/3, 1986/7, 1997/8. However, the nature of interannual variability varies substantially between dataset, possibly with the exception of the period 1988-91 in which there is agreement to within about 0.5 Wm^{-2} . The strongly negative SNLc anomalies for ERA40 during 1985-87 are at odds with SRB and NCEP; these anomalies are smaller for the 24-hour forecast than the 6-hour forecasts. The predominantly negative SNLc anomalies before 1988 and positive anomalies after 1991 for ERA40 are reduced when comparing the 24-hour forecasts with 6-hour forecasts from ERA40; this effectively reduces the positive SNLc heating trend in ERA40 and improves agreement with the empirically derived variability. The derived estimate produces a positive SNLc trend (surface heating) over the period 1979-2004, in contrast to the NCEP data. The ERA40 and NCEP data both simulate a large increase in SNLc during 1997 of about $2\text{-}3 \text{ Wm}^{-2}$ which is approximately double the response derived empirically.

The 0-6 hour and 24-36 hour forecast differences to SRB over the period 1984-94 are similar in nature with positive ERA40 minus SRB differences greater than 10 Wm^{-2} over Africa, India, Australia, Peru and also parts of the south east Pacific and north-equatorial Atlantic. In summary, it is judged that the distribution of SNLc simulated by the 24-36 hour accumulations from ERA40 are similar in quality to the 6-hour forecasts while the 24-36 hour forecasts represent an improved interannual variability. Further comparisons with surface observations are required to demonstrate the robust nature of interannual variability in SNLc.

4.2. Clear-sky Outgoing Longwave Radiation

Time series of low-latitude OLRc over the ocean are presented in Fig. 5. Again, the mean seasonal cycle is removed

from each dataset and a 3-month running mean applied. Despite significant satellite calibration uncertainty, changes in clear-sky sampling due to variable footprint size and variable spatio-temporal sampling, there is good agreement between OLRc anomalies from ERA40 data and the observations, with the possible exception of 1985-86, as found by Allan (2006). Notably, the observed drop in OLRc of about 2 Wm^{-2} from 1998 to 2000 is well captured by ERA40 but not by NCEP. The observed decreasing OLRc trend from 2000-04 is not captured by ERA40 or NCEP. The 24-36 hour forecasts from ERA40 improve agreement with the other datasets compared with the 0-6 hour forecast, in particular with the satellite data over the period 1986-89 and also for the period 1979-83 in comparison with NCEP, including the simulation of the 1982/83 El Niño warm event.

Differences between ERA40 and ERBS over the period 1985-89 are presented in Fig. 6. In addition to the standard clear-sky diagnostics modified OLRc diagnostics (OLR_{cI}) were also calculated from the 6-hourly or 12-hourly accumulations over the period 1985-89; these give greater weighting to cloud-free periods during a month and thereby mimic satellite sampling which only measures emitted radiation from cloud-free regions (e.g. Allan *et al.* 2003):

$$OLR_{cI} = \frac{1}{n} \sum_{h=1}^n \frac{\sum_{d=1}^N OLRc(1 - Ac)}{\sum_{d=1}^N (1 - Ac)}, \quad (1)$$

where h is the hour interval (four 6-hour accumulations per day for the 6 hour forecast or two 12-hour accumulations per day for the 24-36 hour forecasts), d is the day of the month and Ac is the cloud fraction.

As found by Allan *et al.* (2004), ERA40 6-hour forecasts simulate OLRc about 6 Wm^{-2} lower than ERBS over the tropical convective regimes (Fig. 6a). Much of this negative bias was explained by the disparate sampling of clear-skies between the satellite and reanalysis data (Allan and Ringer 2003); indeed, when the ERA40 data are sampled so as to give greater weighting to periods of lower cloud fraction, thereby mimicking satellite sampling, these negative differences mostly disappear and a residual positive ERA40 bias is apparent over much of the mid-latitude and convectively suppressed sub-tropical oceans (Fig. 6b). Similar results are found for the 24-36 hour forecasts from ERA40 (Fig. 6c-d) although differences are generally smaller than for the 6-hour forecast. Since the simulation of OLRc distribution by ERA40 is considered robust (Allan and Ringer 2003), and

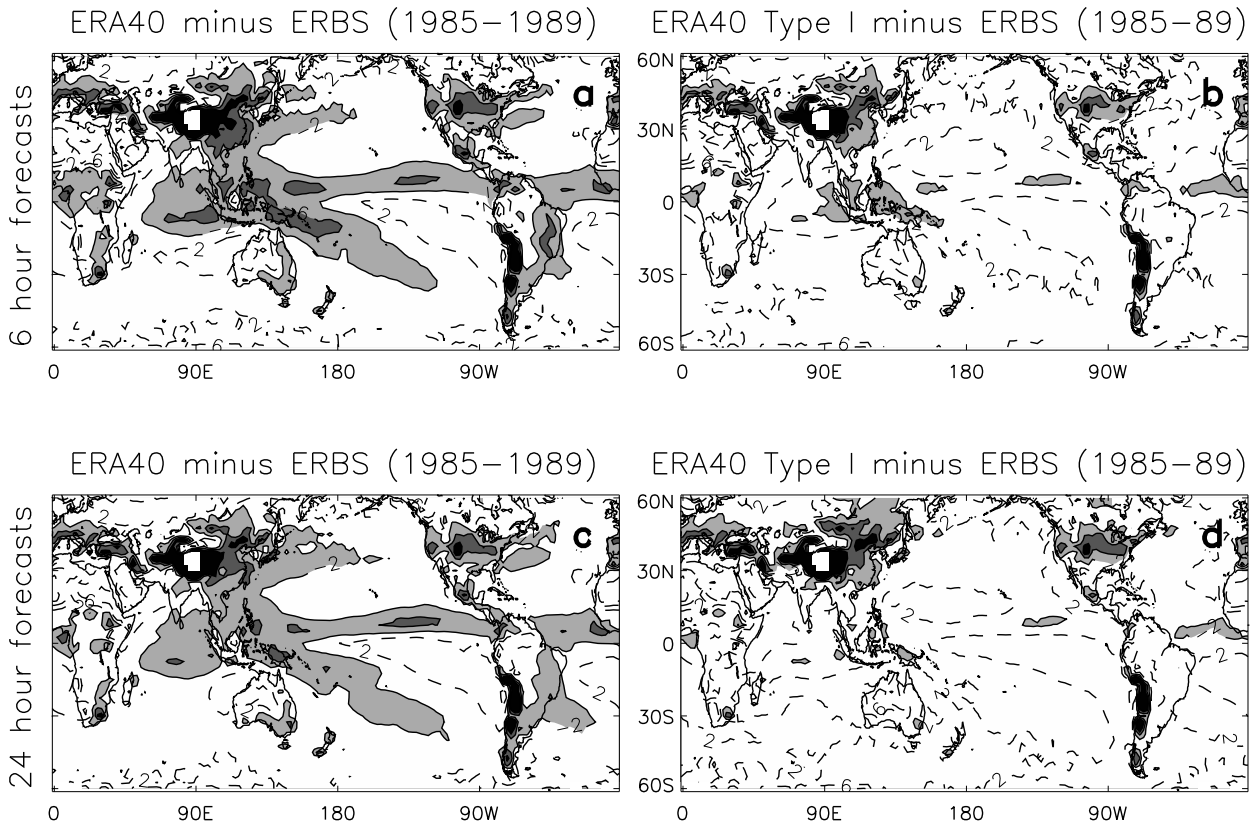


Fig 6. ERA40 minus ERBS clear-sky outgoing longwave radiation (OLRc) differences 1985-89 for (a) ERA40 0-6 hour forecast, (b) ERA40 0-6 hour forecast satellite-like sampling, (c) ERA40 24-36 hour forecast and (d) ERA40 24-36 hour forecast satellite-like sampling. Shading denotes negative differences greater in magnitude than 2 Wm^{-2} ; contours are every 4 Wm^{-2} with solid contours for negative differences and dashed contours for positive differences.

Table 1. Global and low-latitude (40°S - 40°N) ocean mean column integrated water vapour and clear-sky radiation (1979-2001)

Dataset/Domain	CWV (mm)	SNLc (Wm^{-2})	OLRc (Wm^{-2})
Global			
ERA40 6 hr forecast	24.9	-81.6	264.8
ERA40 24 hr forecast	24.5	-82.1	265.2
NCEP	23.9	-85.9	268.6
Low latitude ocean			
ERA40 6 hr forecast	34.5	-75.3	283.9
ERA40 24 hr forecast	33.8	-76.2	284.3
NCEP	33.2	-79.8	287.3

the 24-36 hour forecasts appear to provide still better spatial and temporal comparisons with satellite datasets, these products are well suited to the evaluation of climate models (e.g. Huang *et al.* 2006).

5. Changes in water vapour and clear-sky radiation over land

Since satellite microwave observations of water vapour are available over the ice-free oceans only and OLRc observations are also less likely to be uncertain here due to the ho-

mogeneous surface, less attention has been paid in the evaluation of water vapour and clear-sky radiation over land in reanalyses. Anomaly time series of water vapour and clear-sky radiation are now presented in Fig. 7. It is immediately apparent that agreement between ERA40 and NCEP simulations of CWV and clear-sky radiation is good, in contrast to the oceanic comparisons, in particular for CWV and SNLc. Further, the differences between the 0-6 hour and 24-36 hour simulations from ERA40 are small. These findings suggesting that the spurious water vapour and clear-sky radiation changes in ERA40 are confined to the oceans.

The simulation of SNLc anomalies by SRB contrasts markedly with ERA40 and NCEP (Fig. 7b); this is explained by the likely overestimation of land-surface temperature prior to 1987 which causes negative downward minus upward surface longwave anomalies, also evident in Fig. 4. An overestimation of SRB land surface temperature is also consistent with an overestimation in OLRc anomalies during this period compared with the other datasets considered (Fig. 7c). Agreement between ERA40 OLRc and the satellite observations is less good than over oceans, in particular for the beginning of 1985, and during 1994/5 where the ScaRaB data indicates strongly negative anomalies compared to the ERBS and CERES data. Nevertheless, for the remaining periods of overlap with satellite data, anomalies are within the satellite calibration uncertainty of $\sim 1 \text{ Wm}^{-2}$ (Wielicki *et al.* 2002). Finally, it is interesting to note that the large drop in oceanic OLRc from 1998-2000 seen in the CERES and

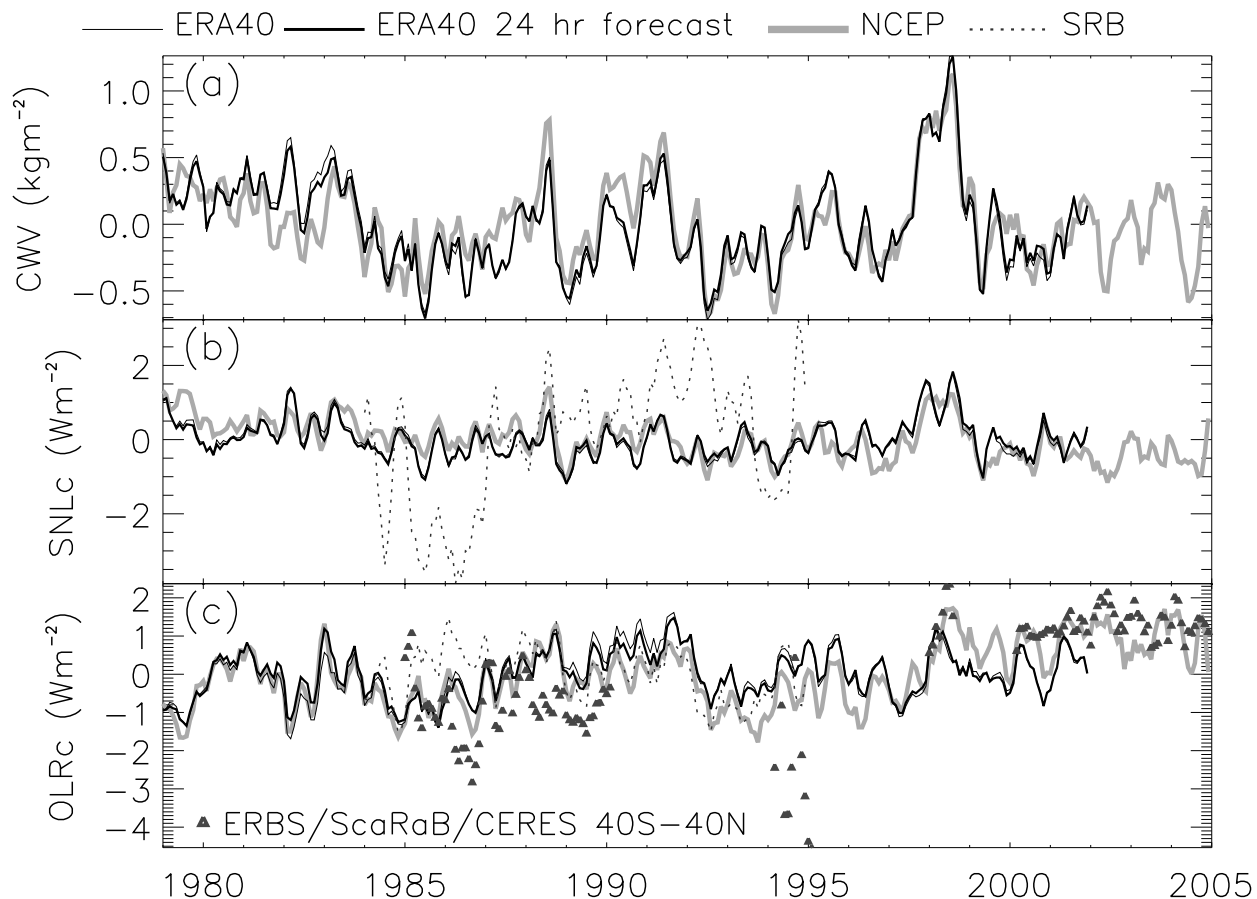


Fig 7. Changes in water vapour and clear-sky radiation over land: (a) column integrated water vapour, (b) clear-sky surface net downward longwave radiation, (c) clear-sky outgoing longwave radiation. The mean seasonal cycle is removed from each time-series and a 3-month running mean applied.

ERA40 data is not apparent over land for either dataset; this merits further analysis.

6. Conclusions

Water vapour and clear-sky radiation simulated by 6 and 24 hour forecasts from ERA40 are compared with other re-analyses, observations and empirical estimates. The global and low-latitude ocean mean values from ERA40 and NCEP are presented in Table 1. The reduction in water vapour from the 6 to the 24-hour ERA40 forecasts explain in part the reduced clear-sky net downward longwave emission to the surface (SNLc) and increase clear-sky emission to space (OLRc), all of which result in closer agreement with NCEP data.

Evaluating the interannual variability and the spatial distribution of water vapour and clear-sky radiation over the 40°N-40°S ocean region it is apparent that overall, the 24 hour forecasts provide a marked improvement over the 6 hour forecasts. Further, the ERA40 24-hour forecast products show better spatio-temporal agreement with satellite observations than the other reanalysis products considered. Therefore, it is recommended that water vapour and clear-sky radiation products from the ERA40 24-hour forecasts are used in preference to other reanalysis products over when

considering the low-latitude ocean regions. Over land, agreement between both ERA40 products and NCEP are good suggesting that the spurious variability found in ERA40 6-hour forecast data is confined to the ocean. Further assessment of water vapour and clear-sky radiation simulated by reanalyses over land is required using ground-based and satellite measurements.

7. Acknowledgments

The input of Adrian Simmons and Igor Zveryaev is gratefully appreciated. IDL software, licensed from the Met Office, was kindly provided by Jonathan Gregory. This work was funded by the NERC grant NE/C51785X/1. The ERA40 data were retrieved from the ECMWF data services; the NCEP data were downloaded from the NOAA-CIRES Climate Diagnostics Center; the SMMR data were extracted from the Jet Propulsion Laboratory DAAC; the SRB, ERBS and CERES data were retrieved from the NASA Langley DAAC; the SSM/I data were retrieved from <http://www.ssmi.com>; the ScaRaB data were provided by the Centre Spatial de Toulouse; the da Silva climatologies were acquired from the International research Institute for Climate and Society LDEO Climate Data Library; the HadISST data were kindly supplied by Nick Rayner.

REFERENCES

- Allan, R. P. (2006). Variability in clear-sky longwave radiative cooling of the atmosphere. *J. Geophys. Res.*, **in press**, doi:10.1029/2006JD007304.
- Allan, R. P. and Ringer, M. A. (2003). Inconsistencies between satellite estimates of longwave cloud forcing and dynamical fields from reanalyses. *Geophys. Res. Lett.*, **30**, 1491, doi 10.1029/2003GL017019.
- Allan, R. P., Ringer, M. A., and Slingo, A. (2003). Evaluation of moisture in the Hadley Centre climate model using simulations of HIRS water-vapour channel radiances. *Quart. J. Roy. Meteorol. Soc.*, **129**, 3371–3389.
- Allan, R. P., Ringer, M. A., Pament, J. A., and Slingo, A. (2004). Simulation of the Earth's radiation budget by the European Centre for Medium Range Weather Forecasts 40-year reanalysis (ERA40). *J. Geophys. Res.*, **109**(D05105), doi:10.1029/2004JD005232.
- da Silva, A., Young, A. C., and Levitus, S. (1994). Atlas of surface marine data 1994, volume 1: Algorithms and procedures. Technical Report 6, NESDIS, U.S. Department of Commerce, Washington, D.C.
- Huang, X., Ramaswamy, V., and Schwarzkopf, D. (2006). Quantification of the source of errors in AM2 simulated tropical clear-sky outgoing longwave radiation. *J. Geophys. Res.*, **111**, D14107, doi:10.1029/2005JD006576.
- Kalnay, E., Kanamitsu, M., Kistler, R., Collins, W., Deaven, D., Gandin, L., Irdell, M., Saha, S., White, G., Woollen, J., Zhu, Y., Chelliah, M., Ebisuzaki, W., Higgins, W., Janowiak, J., Mo, K. C., Ropelewski, C., Wang, J., Leetmaa, A., Reynolds, R., Jenne, R., and Joseph, D. (1996). The NCEP/NCAR 40-year reanalysis project. *Bull. Amer. Met. Soc.*, **77**, 437–471.
- Prata, A. J. (1996). A new longwave formula for estimating downwelling clear sky radiation at the surface. *Quart. J. Roy. Meteorol. Soc.*, **122**, 1127–1151.
- Rayner, N. A., Parker, D., Horton, E., Folland, C., Alexander, L., Rowell, D., Kent, E., and Kaplan, A. (2003). Global analysis of sst, sea ice and night marine air temperature since the late nineteenth century. *J. Geophys. Res.*, **108**, 4407, doi:10.1029/2002JD002670.
- Stackhouse, P. W. J., Cox, S. J., Gupta, S. K., Dipasquale, R. C., and Brown, D. E. (1999). The WCRP/GEWEX Surface Radiation Budget Project Release 2: first results at 1 degree resolution. 10th Conf. on Atmospheric Radiation, Madison, WI. Amer. Meteor. Soc.
- Stephens, G. L., Slingo, A., Webb, M. J., Minnett, P. J., Daum, P. H., Kleinman, L., Wittmeyer, I., and Randall, D. A. (1994). Observations of the earth's radiation budget in relation to atmospheric hydrology 4. atmospheric column radiative cooling over the world's oceans. *J. Geophys. Res.*, **99**, 18585–18604.
- Trenberth, K. E., Fasullo, J., and Smith, L. (2005). Trends and variability in column-integrated atmospheric water vapor. *Climate Dynamics*, **24**, 741 – 758.
- Uppala, S. M., Kallberg, P. W., Simmons, A. J., Andrae, U., da Costa Bechtold, V., Fiorino, M., Gibson, J. K., Haseler, J., Hernandez, A., Kelly, G. A., Li, X., Onogi, K., Saarinen, S., Sokka, N., Allan, R. P., Andersson, E., Arpe, K., Balmaseda, M. A., Beljaars, A. C. M., van de Berg, L., Bidlot, J., Bormann, N., Caires, S., Chevallier, F., Dethof, A., Dragosavac, M., Fisher, M., Fuentes, M., Hagemann, S., Holm, E., Hoskins, B., Isaksen, I., Janssen, P. A. E. M., Jenne, R., McNally, A. P., Mahfouf, J. F., Morcrette, J. J., Rayner, N. A., Saunders, R. W., Simon, P., Sterl, A., Trenberth, K. E., Untch, A., Vasiljevic, D., Viterbo, P., and Woollen, J. (2005). The ERA-40 reanalysis. *Quart. J. Roy. Meteorol. Soc.*, **131**, 2961–3012.
- Wentz, F. J. (1997). A well-calibrated ocean algorithm for SMM/I. *J. Geophys. Res.*, **102**(C4), 8703–8718.
- Wentz, F. J. and Francis, E. A. (1992). Nimbus-7 SMMR ocean products, 1979-1984. Technical report, Remote Sensing Systems Tech. Rep. 033192, 36 pp. [Available from Remote Sensing Systems, 1101 College Ave., Santa Rosa, CA 95404].
- Wielicki, B. A., Wong, T., Allan, R. P., Slingo, A., Kiehl, J. T., Soden, B. J., Gordon, C. T., Miller, A. J., Yang, S., Randall, D. A., Robertson, F., Susskind, J., and Jacobowitz, H. (2002). Evidence for large decadal variability in the tropical mean radiative energy budget. *Science*, **295**, 841–844.